Published OnlineFirst October 20, 2020; DOI: 10.1158/1055-9965.EPI-20-0889

Collagen Organization in Relation to Ductal Carcinoma *In Situ* Pathology and Outcomes

Brian L. Sprague[1,2,3], Pamela M. Vacek[2,4], Sophie E. Mulrow[1], Mark F. Evans[2,5], Amy Trentham-Dietz[6,7], Sally D. Herschorn[2,3], Ted A. James[8], Nuntida Surachaicharn[9], Adib Keikhosravi[10], Kevin W. Eliceiri[7,10], Donald L. Weaver[2,5], and Matthew W. Conklin[7,9]

ABSTRACT

Background: There is widespread interest in discriminating indolent from aggressive ductal carcinoma *in situ* (DCIS). We sought to evaluate collagen organization in the DCIS tumor microenvironment in relation to pathologic characteristics and patient outcomes.

Methods: We retrieved fixed tissue specimens for 90 DCIS cases within the population-based Vermont DCIS Cohort. We imaged collagen fibers within 75 μm of the tumor/stromal boundary on hematoxylin and eosin–stained slides using multiphoton microscopy with second-harmonic generation. Automated software quantified collagen fiber length, width, straightness, density, alignment, and angle to the tumor/stroma boundary. Factor analysis identified linear combinations of collagen fiber features representing composite attributes of collagen organization.

Results: Multiple collagen features were associated with DCIS grade, necrosis pattern, or periductal fibrosis ($P < 0.05$). After adjusting for treatments and nuclear grade, risk of recurrence (defined as any second breast cancer diagnosis) was lower among cases with greater collagen fiber width [hazard ratio (HR), 0.57 per one standard deviation increase; 95% confidence interval (CI), 0.39–0.84] and fiber density (HR, 0.60; 95% CI, 0.42–0.85), whereas risk was elevated among DCIS cases with higher fiber straightness (HR, 1.47; 95% CI, 1.05–2.06) and distance to the nearest two fibers (HR, 1.47; 95% CI, 1.06–2.02). Fiber length, alignment, and fiber angle were not associated with recurrence ($P > 0.05$). Five composite factors were identified, accounting for 72.4% of the total variability among fibers; three were inversely associated with recurrence (HRs ranging from 0.60 to 0.67; $P \leq 0.01$).

Conclusions: Multiple aspects of collagen organization around DCIS lesions are associated with recurrence risk.

Impact: Collagen organization should be considered in the development of prognostic DCIS biomarker signatures.

Introduction

Ductal carcinoma *in situ* (DCIS) is considered the earliest form of breast cancer, in which malignant cells are confined within the basement membrane of the breast duct system (1). DCIS is typically detected by mammography and accounts for >25% of screen-detected breast cancers (2). DCIS is considered a non-obligate precursor to invasive breast cancer (3). Because of uncertainty in the natural history of DCIS (4–10), there is widespread concern regarding overtreatment (11). It is not currently possible to determine which DCIS lesions are likely to progress to a potentially lethal-invasive stage; thus, most women diagnosed with DCIS undergo surgical, radiation, and endocrine hormone therapies similar to women diagnosed with invasive breast cancer (12). Identification of DCIS prognostic markers could permit personalized treatment strategies that spare women unnecessary treatments (3). Most prior research on DCIS biomarkers has focused on the malignant epithelial cancer cells: their genetic characteristics, protein- and RNA-expression, morphology, and growth patterns (13–15). Chromosomal abnormalities in DCIS are remarkably similar to invasive carcinoma (16). This suggests that other factors are involved in DCIS progression.

Several lines of evidence suggest that the surrounding stromal tissue is an active and necessary accomplice in promoting invasion (17–21). Collagen is a major component of the stromal tissue that surrounds breast ducts. Laboratory studies have shown that fibrillar collagen plays a key role in promoting tumor initiation and metastasis (22). Prior studies have suggested that collagen fiber orientation and alignment are prognostic markers in patients with invasive breast cancer (23, 24). We previously found that collagen fiber alignment in DCIS specimens was associated with poor prognosis pathology characteristics, but not with recurrence (1). To our knowledge, other aspects of collagen organization have not been evaluated in DCIS specimens. We sought to comprehensively characterize collagen structural organization around DCIS lesions and evaluate its association with DCIS pathology and outcomes within a well-characterized population-based cohort.

[1]Department of Surgery, Office of Health Promotion Research, University of Vermont Larner College of Medicine, Burlington, Vermont. [2]University of Vermont Cancer Center, University of Vermont Larner College of Medicine, Burlington, Vermont. [3]Department of Radiology, University of Vermont Larner College of Medicine, Burlington, Vermont. [4]Department of Medical Biostatistics, University of Vermont, Burlington, Vermont. [5]Department of Pathology and Laboratory Medicine, University of Vermont Larner College of Medicine, Burlington, Vermont. [6]Department of Population Health Sciences, University of Wisconsin–Madison, Madison, Wisconsin. [7]Carbone Cancer Center, School of Medicine and Public Health, University of Wisconsin–Madison, Madison, Wisconsin. [8]Department of Surgery, Beth Israel Deaconess Medical Center, Harvard Medical School, Boston, Massachusetts. [9]Department of Cell and Regenerative Biology, University of Wisconsin–Madison, Madison, Wisconsin. [10]Department of Biomedical Engineering, Laboratory for Optical and Computations Instrumentation, University of Wisconsin–Madison, Madison, Wisconsin.

Note: Supplementary data for this article are available at Cancer Epidemiology, Biomarkers & Prevention Online (http://cebp.aacrjournals.org/).

D.L. Weaver and M.W. Conklin contributed equally as co-senior authors of this article.

Corresponding Authors: Brian L. Sprague, University of Vermont, 1 South Prospect Street, Burlington, VT 05405. Phone: 802-656-4112; E-mail: Brian.Sprague@uvm.edu; and Matthew W. Conklin, Room 4537 WIMR II, 1111 Highland Avenue, University of Wisconsin–Madson, Madison WI 53705. Phone: 608-263-8465; E-mail: mwconklin@wisc.edu

Cancer Epidemiol Biomarkers Prev 2021;30:80–8

doi: 10.1158/1055-9965.EPI-20-0889

Published OnlineFirst October 20, 2020; DOI: 10.1158/1055-9965.EPI-20-0889

Materials and Methods

Study population

The Vermont DCIS cohort (25) includes 1,252 women diagnosed with DCIS in Vermont during 1994–2012, identified via the Vermont Breast Cancer Surveillance System (VBCSS). The VBCSS is one of six active breast imaging registries within the Breast Cancer Surveillance Consortium (26, 27) and collects breast imaging data from all radiology facilities in Vermont, linked to pathology records and the Vermont Cancer Registry (28, 29). This study was approved by the University of Vermont Institutional Review Board with a waiver of consent.

The Vermont DCIS cohort includes women diagnosed with DCIS as a first primary breast cancer (25). Women with a concurrent invasive breast cancer diagnosis are excluded. For this study, a roster of 148 DCIS cases was initially identified from the Vermont DCIS Cohort. This included 74 patients who had experienced a second event [defined as any second breast cancer diagnosis (*in situ* or invasive, ipsilateral or contralateral)] occurring at least 6 months after the initial DCIS diagnosis and 74 who had not experienced a second event. Ultimately, adequate tissue specimens for collagen fiber analysis were available for 90 cases, including 51 who experienced a second event and 39 who had not (**Table 1**). Reasons for unavailability of tissue specimens included: pathology facility no longer retained the tissue specimen (e.g., for cases >15 years old at certain facilities), no DCIS remained in the tissue specimen, or the case was released for other research and paraffin blocks could not be located.

Clinical data

All participants completed a questionnaire at breast imaging visits, providing information on demographics and treatment information. Radiological exam results reported by the radiology facility included indication (i.e., screening vs. diagnostic) and assessments, which were used to determine the DCIS method of detection (30). Pathology reports for all breast specimens evaluated at pathology facilities in Vermont were linked to study participants, with standardized data abstracted on specimen type and histology. Pathology slides and blocks for the index DCIS were reviewed centrally by a single pathologist (D.L. Weaver) to confirm the diagnosis and record standardized data on nuclear grade, necrosis, inflammation, and periductal fibrosis. Among the 73 cases with grade available from clinical pathology reports, there was 81% agreement with grade from the central review. Participants were also linked to the Vermont Cancer Registry, providing consolidated information on stage at diagnosis and treatment data.

Treatment was categorized on the basis of the clinical questionnaire, pathology record, and cancer registry data, as previously described (25). Data from subsequent pathology reports and the Vermont Cancer Registry were used to identify second breast cancer diagnoses occurring ≥6 months after the index DCIS diagnosis. Second events included DCIS or invasive breast cancer diagnosed in the ipsilateral or contralateral breast.

Table 1. Characteristics of study participants from the Vermont DCIS Cohort.

Characteristics	*N*	(%)
Age at diagnosis		
<50	36	40.0
50–69	40	44.4
70+	14	15.6
Mode of detection		
Screening	62	68.9
Symptoms	13	14.4
Missing	15	16.7
Treatment		
Mastectomy	5	5.6
BCS only	38	42.2
BCS and radiotherapy	26	28.9
BCS and endocrine therapy	9	10.0
BCS and radiotherapy and endocrine therapy	12	13.3
Recurrence		
No	39	43.3
Yes-ipsilateral	38	42.2
Yes-contralateral	12	13.3
Yes-bilateral	1	1.1
Type of recurrence		
None	39	43.3
DCIS	25	27.8
Invasive breast cancer	26	28.9

Abbreviation: BCS, breast conserving surgery.

Collagen assessment

The study pathologist (D.L. Weaver) identified a representative tumor block to re-cut a hematoxylin and eosin–stained slide for collagen analysis. The slide was digitized and annotated by the pathologist to identify areas of DCIS. Specific imaging locations within these relatively large areas were chosen by the microscopist (M.W. Conklin) based on the criteria that they include adequate stromal collagen that could be clearly ascribed to a specific DCIS tumor/stromal boundary, without interference from blood vessels, fatty areas, or non-annotated areas of epithelium. The microscopist was blinded to the cases' recurrence status. One to five 770 × 770-μm locations were imaged per case, with 91% of cases having ≥3 locations imaged. Second-harmonic generation (SHG) on a multiphoton microscope (see detailed imaging protocol in the Supplementary Methods) was used to image collagen fibers. The frequency doubling of the incident laser light caused by the unique tertiary structure of collagen allows for this, producing an image of only collagen fibers (**Fig. 1**). To alleviate out of focal plane issues due to the unevenness of the tissue slice, 3 z-planes were captured per SHG image and then maximum-intensity projected to capture the entire axial field of view. The open-source image analysis software packages CT-FIRE and CurveAlign were used to quantify collagen fiber features, as previously described (24, 31–33). CT-Fire determined the total length (i.e., following the contour of the fiber), end-to-end length (i.e., straight distance between one end of the fiber to the other end), and width of each collagen fiber in the SHG image. The ratio of end-to-end length to total length was computed as a measure of straightness, and the difference between total and end-to-end length was computed as another measure of the fiber's curviness. CurveAlign measured fiber alignment, fiber density, distance to the nearest two fibers, and the angle of fibers with respect to the tumor/stromal boundary, as previously described (34). Briefly, fiber alignment (i.e., anisotropy) is calculated as coefficients ranging from 0 to 1, with 1 indicating perfectly aligned fibers and 0 representing randomly oriented fibers. Fiber density was defined on three different scales: counts of fibers within a 24, 48, or 96-μm square box centered on the fiber centroid. All collagen measures used in analyses were restricted to fibers within 100 pixels (75.19 μm) from the tumor/stromal boundary. A brief summary of the definitions of each collagen feature used in the study is provided in Supplementary Table S1. A detailed description of the computational methods used to make these measurements, along with a

Published OnlineFirst October 20, 2020; DOI: 10.1158/1055-9965.EPI-20-0889

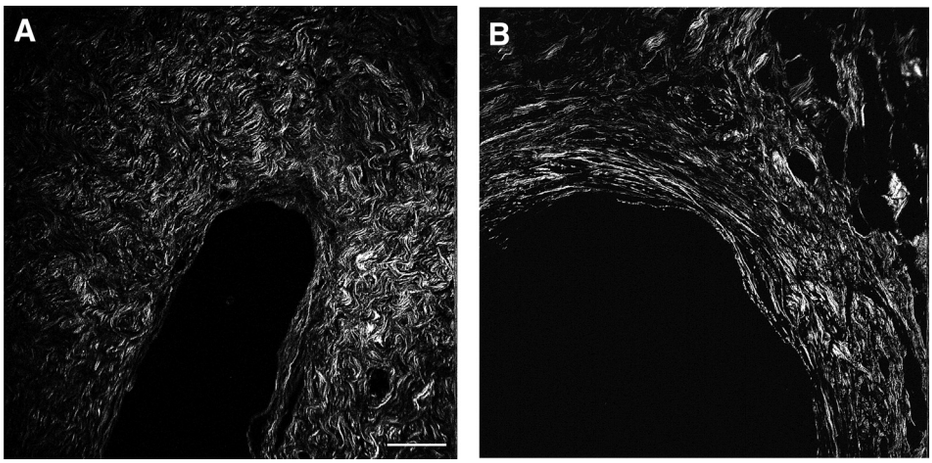

Figure 1.
Sample multiphoton microscopy images of collagen fibers, illustrating cases with different collagen features. **A,** Shows an area of DCIS surrounded by short, curvy, dense fibers. **B,** Shows an area of DCIS surrounded with long, straight, high-alignment fibers; scale bar, 100 μm.

validation of their accuracy using a synthetic test set of fibers has been previously published (35).

Statistical analysis

Summary statistics were used to describe the distribution of collagen features of individual fibers across imaged locations and their mean values for each woman were computed. Factor analysis was performed on a set of 11 collagen features of each fiber to identify linear combinations that account for the covariance among features and potentially represent composite attributes of collagen organization. The principal component factoring method was used, and five factors with eigenvalues greater than 1.0 were retained. Varimax rotation was used to obtain orthogonal factors. Values of the five factors were computed for each fiber, and the mean value determined across all fibers from each woman. Associations of collagen features and factor scores with DCIS pathology characteristics were examined by ANOVA. Cox regression was used to assess associations of collagen features and factor scores with time to occurrence of a second breast cancer event, adjusted for nuclear grade and treatment. In sensitivity analyses, we adjusted for additional variables, including age, menopausal status, body mass index, breast density, method of detection, and surgical margin status. Disease-free survival was defined as the time from diagnosis to a second breast cancer diagnosis, with censoring at the date of the last VBCSS breast imaging or pathology record. All statistical analyses were performed in SAS Version 9.4 (SAS Institute Inc.), all tests were two-sided, and P values ≤0.05 were considered statistically significant.

Results

Forty percent of the participants were under age 50 at diagnosis, and 42% were treated only with breast-conserving surgery (**Table 1**). The majority of second events (74.5%) occurred in the ipsilateral breast, and approximately half of second breast cancer diagnoses were invasive. The mean time to second event was 5.4 years (range, 0.5–15.3 years); mean follow-up time among cases without a second event was 12.7 years (range, 2.4–20.9 years).

Collagen fiber features

37,523 fibers were identified among the 90 imaged DCIS lesions. All collagen features were highly variable except fiber straightness, which is a ratio of two highly correlated measures and had a coefficient of variation (CV) across all fibers and women of 5.5%. CVs for all other collagen features ranged from 19% to 92% (Supplementary Table S2). For all features, differences between fibers within an imaged location accounted for most of the variability (88.1% to 98.6% of the total variance). Differences between locations within a woman's DCIS sample contributed 0.6% to 9.5% to the total variance, whereas differences between women contributed 0.2% to 5.3%. Despite the between-fiber variation in individual features, differing patterns of collagen organization were evident among women (**Fig. 1**).

Four fiber features were inversely related to DCIS nuclear grade and necrosis pattern: total minus end-to-end length, width, box density 48 × 48 μm, and box density 96 × 96 μm (**Table 2**). Distance to the nearest two fibers was positively associated with nuclear grade and necrosis pattern. Straightness, box density 24 × 24 μm, alignment of the nearest 4 fibers, and angle to the tumor/stromal boundary were associated with necrosis pattern but not nuclear grade. The presence of inflammation was associated with a smaller difference between fiber total length and end-to-end length, greater straightness, more narrow fiber width, and higher alignment to the nearest four fibers. Only total minus end-to-end fiber length was significantly related to periductal fibrosis, with lower values observed for DCIS lesions having concentric cellular fibrosis.

Composite measures

Factor analysis identified five linear combinations of 11 collagen features (factors) that accounted for 72.4% of the total variability of the features among fibers. The standardized scoring coefficients for computing factor scores are shown in **Table 3** and provide insight into the collagen attribute being measured by indicating the relative strength of the correlation (loading) between each fiber feature and factor score. These relationships are also summarized in Supplementary Table S1. Factor 1 loaded positively on box density 24 × 24 μm and negatively on box alignment 24 × 24 μm, such that cases with high values of Factor 1 had localized areas of collagen with a high density of non-aligned fibers. Factor 2 loaded most highly on box density 96 × 96 μm and distance from the tumor/stromal boundary, indicating areas of dense collagen closer to the outer boundary of the area measured (75.19 μm) from the tumor/stromal boundary. Total minus end-to-end fiber length and straightness loaded positively and negatively on Factor 3, respectively, indicative of curved or serpentine fibers. Factor 4 loaded positively on alignment of the nearest four fibers and negatively

Published OnlineFirst October 20, 2020; DOI: 10.1158/1055-9965.EPI-20-0889

Table 2. Association between collagen features and DCIS pathology characteristics, Vermont DCIS Cohort.

	N	Total length (μm)	Total minus end-to-end length (μm)	Straightness[a]	Width (μm)	Distance to nearest 2 fibers (μm)	Box density 24 × 24 μm[b]	Box density 48 × 48 μm[b]	Box density 96 × 96 μm[b]	Alignment of nearest 4	Box alignment 24 × 24 μm[c]	Distance to tumor/ stromal boundary (μm)	Angle to tumor/ stromal boundary (°)
Nuclear grade		Mean (SE)	Mean (SE)	Mean (SE)	Mean (SE)	Mean (SE)	Mean (SE)	Mean (SE)	Mean (SE)	Mean (SE)	Mean (SE)	Mean (SE)	Mean (SE)
Low	7	41.63 (0.60)	**3.55 (0.11)**	0.916 (0.002)	**3.33 (0.09)**	**21.06 (0.68)**	1.41 (0.04)	**3.30 (0.19)**	**10.62 (0.79)**	0.705 (0.025)	0.918 (0.012)	38.82 (0.83)	25.67 (1.82)
Intermediate	45	42.54 (0.45)	**3.53 (0.05)**	0.918 (0.001)	**3.20 (0.02)**	**21.67 (0.30)**	1.39 (0.01)	**3.19 (0.06)**	**10.21 (0.23)**	0.738 (0.009)	0.928 (0.004)	37.93 (0.30)	23.25 (0.61)
High	36	41.98 (0.53)	**3.37 (0.05)**	0.920 (0.001)	**3.08 (0.02)**	**23.17 (0.38)**	1.36 (0.01)	**2.96 (0.06)**	**9.19 (0.25)**	0.756 (0.010)	0.935 (0.005)	38.13 (0.30)	22.67 (0.69)
		$P = 0.62$	$\mathbf{P = 0.02}$	$P = 0.18$	$\mathbf{P < 0.001}$	$\mathbf{P = 0.007}$	$P = 0.17$	$\mathbf{P = 0.01}$	$\mathbf{P = 0.01}$	$P = 0.10$	$P = 0.31$	$P = 0.59$	$P = 0.23$
Necrosis													
Absent	25	42.64 (0.60)	**3.57 (0.05)**	**0.918 (0.001)**	**3.28 (0.04)**	**21.21 (0.38)**	**1.42 (0.02)**	**3.30 (0.08)**	**10.60 (0.34)**	**0.724 (0.014)**	0.920 (0.008)	38.67 (0.45)	**24.57 (0.95)**
Focal	21	40.95 (0.60)	**3.52 (0.07)**	**0.915 (0.002)**	**3.14 (0.04)**	**21.98 (0.45)**	**1.38 (0.02)**	**3.13 (0.08)**	**10.00 (0.34)**	**0.718 (0.013)**	0.928 (0.006)	37.85 (0.38)	**24.41 (0.88)**
Central necrosis	41	42.61 (0.45)	**3.38 (0.04)**	**0.921 (0.001)**	**3.10 (0.02)**	**23.03 (0.38)**	**1.36 (0.01)**	**2.97 (0.05)**	**9.25 (0.23)**	**0.767 (0.007)**	0.937 (0.004)	37.84 (0.30)	**21.79 (0.55)**
		$P = 0.10$	$\mathbf{P = 0.01}$	$\mathbf{P = 0.003}$	$\mathbf{P < 0.001}$	$\mathbf{P = 0.009}$	$\mathbf{P = 0.03}$	$\mathbf{P = 0.003}$	$\mathbf{P = 0.004}$	$\mathbf{P = 0.002}$	$P = 0.07$	$P = 0.27$	$\mathbf{P = 0.01}$
Inflammation													
Present	32	42.57 (0.53)	**3.37 (0.05)**	**0.921 (0.001)**	**3.11 (0.03)**	22.72 (0.38)	1.37 (0.01)	3.04 (0.07)	9.54 (0.27)	**0.760 (0.011)**	0.936 (0.005)	38.17 (0.30)	22.67 (0.80)
Absent	56	42.05 (0.38)	**3.53 (0.04)**	**0.917 (0.001)**	**3.19 (0.02)**	21.96 (0.30)	1.39 (0.01)	3.14 (0.05)	9.99 (0.22)	**0.733 (0.008)**	0.927 (0.004)	38.04 (0.23)	23.51 (0.54)
		$P = 0.45$	$\mathbf{P = 0.01}$	$\mathbf{P = 0.01}$	$\mathbf{P = 0.05}$	$P = 0.15$	$P = 0.29$	$P = 0.24$	$P = 0.21$	$\mathbf{P = 0.04}$	$P = 0.19$	$P = 0.78$	$P = 0.37$
Periductal fibrosis													
No	39	42.55 (0.53)	**3.50 (0.05)**	0.919 (0.001)	3.19 (0.03)	22.37 (0.38)	1.37 (0.02)	3.07 (0.07)	9.74 (0.30)	0.743 (0.011)	0.933 (0.006)	37.78 (0.30)	23.08 (0.70)
Yes-concentric/ not cellular	6	42.41 (0.75)	**3.65 (0.13)**	0.914 (0.002)	3.15 (0.05)	21.71 (0.98)	1.42 (0.02)	3.16 (0.15)	10.12 (0.63)	0.742 (0.011)	0.920 (0.005)	38.41 (0.60)	22.95 (1.57)
Yes-concentric/ cellular	31	41.84 (0.45)	**3.36 (0.05)**	0.920 (0.001)	3.11 (0.02)	22.57 (0.38)	1.37 (0.01)	3.06 (0.05)	9.59 (0.24)	0.753 (0.010)	0.932 (0.005)	38.38 (0.30)	22.90 (0.80)
Yes-other[d]	10	42.52 (0.68)	**3.62 (0.06)**	0.917 (0.002)	3.19 (0.06)	21.37 (0.60)	1.40 (0.03)	3.28 (0.10)	10.37 (0.39)	0.723 (0.015)	0.922 (0.008)	38.08 (0.68)	24.00 (1.04)
		$P = 0.81$	$\mathbf{P = 0.01}$	$P = 0.16$	$P = 0.24$	$P = 0.53$	$P = 0.61$	$P = 0.39$	$P = 0.56$	$P = 0.62$	$P = 0.60$	$P = 0.69$	$P = 0.92$

Note: *P* values were computed from ANOVA tests of whether the mean collagen feature differed among groups based on the DCIS pathology characteristic. *P* values less than 0.05 were considered statistically significant and are indicated in bold font.

Abbreviation: SE, standard error.

[a]Straightness is defined as the ratio of the end-to-end length to the total length of the fiber.

[b]Box density refers to the number of collagen fibers contained within box of the specified size overlaid on the fiber centroid.

[c]Alignment of fibers contained within a 24 × 24-μm box overlaid on the fiber centroid.

[d]Includes periductal fibrosis that is neither cellular nor concentric, as well as periductal fibrosis with unknown concentricity/cellularity.

Published OnlineFirst October 20, 2020; DOI: 10.1158/1055-9965.EPI-20-0889

Table 3. Standardized scoring coefficients for computing composite measures identified from factor analysis, Vermont DCIS Cohort.

	Factor 1	Factor 2	Factor 3	Factor 4	Factor 5
Total length	0.048	−0.143	0.195	0.117	**0.482**
Total minus end-to-end length	0.006	−0.026	**0.489**	0.005	0.092
Straightness[a]	0.038	−0.087	**−0.487**	0.077	0.291
Width (μm)	−0.071	0.083	−0.141	−0.137	**0.675**
Distance to nearest 2 fibers	−0.244	−0.197	0.007	−0.190	0.025
Box density 24 × 24 μm[b]	**0.478**	−0.139	0.011	0.051	−0.034
Box density 48 × 48 μm[b]	0.158	0.270	−0.010	0.130	−0.035
Box density 96 × 96 μm[b]	−0.055	**0.424**	0.001	0.043	0.058
Alignment of the nearest 4 fibers	0.004	0.103	−0.012	**0.591**	−0.220
Box alignment 24 × 24 μm[c]	**−0.424**	0.226	0.007	0.236	−0.035
Distance to tumor/stromal boundary (μm)	−0.286	**0.438**	0.031	−0.162	−0.040
Angle relative to tumor/stromal boundary (°)	−0.046	0.052	0.023	**−0.479**	−0.119

Note: Bold font is used to highlight collagen features with the highest coefficients (absolute value >0.4).
[a]Straightness is defined as the ratio of the end-to-end length to the total length of the fiber.
[b]Box density refers to the number of collagen fibers contained within a box of the specified size overlaid on the fiber centroid.
[c]Alignment of fibers contained within a 24 × 24-μm box overlaid on the fiber centroid.

on angle to the tumor/stromal boundary, indicating the presence of aligned fibers that tended to be parallel to the tumor boundary. Factor 5 loaded most heavily on fiber length and width.

Mean values of factors 2 and 5, averaged across all fibers for each woman, had inverse relationships with nuclear grade (**Table 4**). All five factors were associated with necrosis patterns. Only Factor 3 was significantly associated with inflammation and periductal fibrosis.

Associations with risk of recurrence

Risk of a second breast cancer event was related to several fiber features as well as three of the factors (**Table 5**). After adjusting for treatments and nuclear grade, risk of any second event was lower among cases with greater collagen fiber width [HR, 0.57 per one standard deviation increase; 95% confidence interval (CI), 0.39–0.84] and fiber density within a 96 × 96 μm box (HR, 0.60;

Table 4. Association of collagen composite factors with DCIS pathology characteristics, Vermont DCIS Cohort.

		Mean factor value (SE)				
	N	Factor 1 (high density, low alignment)	Factor 2 (high density, long distance to tumor/stromal boundary)	Factor 3 (serpentine, not straight)	Factor 4 (high alignment, parallel orientation to tumor boundary)	Factor 5 (long, wide fibers)
Nuclear grade						
Low	7	0.27 (0.35)	**0.53 (0.45)**	−0.04 (0.45)	−0.62 (0.42)	**0.82 (0.48)**
Intermediate	45	0.15 (0.14)	**0.20 (0.14)**	0.13 (0.15)	0.02 (0.15)	**0.23 (0.15)**
High	36	−0.28 (0.16)	**−0.38 (0.15)**	−0.18 (0.16)	0.15 (0.16)	**−0.46 (0.13)**
		$P = 0.10$	$\mathbf{P = 0.01}$	$P = 0.36$	$P = 0.18$	$\mathbf{P < 0.001}$
Necrosis						
Absent	25	**0.35 (0.22)**	**0.47 (0.20)**	**0.08 (0.19)**	**−0.25 (0.23)**	**0.64 (0.20)**
Focal	21	**0.04 (0.19)**	**0.07 (0.20)**	**0.41 (0.22)**	**−0.32 (0.22)**	**−0.24 (0.21)**
Central necrosis	41	**−0.27 (0.14)**	**−0.35 (0.14)**	**−0.27 (0.14)**	**0.36 (0.12)**	**−0.32 (0.13)**
		$\mathbf{P = 0.04}$	$\mathbf{P = 0.004}$	$\mathbf{P = 0.03}$	$\mathbf{P = 0.01}$	$\mathbf{P < 0.001}$
Inflammation						
Present	32	−0.19 (0.16)	−0.17 (0.17)	**−0.30 (0.16)**	0.25 (0.18)	−0.24 (0.16)
Absent	56	0.08 (0.14)	0.08 (0.14)	**0.16 (0.13)**	−0.11 (0.13)	0.12 (0.14)
		$P = 0.21$	$P = 0.26$	$\mathbf{P = 0.03}$	$P = 0.10$	$P = 0.10$
Periductal fibrosis						
No	39	−0.11 (0.18)	−0.07 (0.18)	**0.00 (0.16)**	0.01 (0.18)	0.17 (0.19)
Yes, concentric, not cellular	6	0.32 (0.30)	0.13 (0.39)	**0.80 (0.34)**	0.05 (0.23)	−0.13 (0.28)
Yes, concentric and cellular	31	−0.11 (0.13)	−0.12 (0.15)	**−0.29 (0.16)**	0.14 (0.18)	−0.33 (0.14)
Yes, other[a]	10	0.33 (0.28)	0.30 (0.25)	**0.40 (0.21)**	−0.16 (0.25)	0.21 (0.33)
		$P = 0.46$	$P = 0.66$	$\mathbf{P = 0.03}$	$P = 0.87$	$P = 0.19$

Note: *P* values were computed from ANOVA tests of whether the mean collagen composite factor differed among groups based on the DCIS pathology characteristic. *P* values less than 0.05 were considered statistically significant and are indicated in bold font.
Abbreviation: SE, standard error.
[a]Includes periductal fibrosis that is neither cellular nor concentric, as well as periductal fibrosis with unknown concentricity/cellularity.

Published OnlineFirst October 20, 2020; DOI: 10.1158/1055-9965.EPI-20-0889

Table 5. Associations between collagen organization and risk of recurrence, Vermont DCIS Cohort. All hazard ratios correspond to an increase of one standard deviation in the collagen measure.

	Any second event				Ipsilateral second event			
	Adjusted for treatment		Adjusted for treatment and grade		Adjusted for treatment		Adjusted for treatment and grade	
	HR (95% CI)	*P*	HR (95% CI)	*P*	HR (95% CI)	*P*	HR (95% CI)	*P*
Directly measured collagen features								
Total length	0.76 (0.54–1.06)	0.10	0.77 (0.55–1.08)	0.13	0.74 (0.50–1.10)	0.14	0.74 (0.50–1.10)	0.13
Total minus end-to-end length	**0.51 (0.36–0.71)**	**<0.001**	**0.55 (0.39–0.76)**	**<0.001**	**0.53 (0.37–0.76)**	**<0.001**	**0.57 (0.39–0.82)**	**0.003**
Straightness[a]	**1.52 (1.09–2.10)**	**0.01**	**1.47 (1.05–2.06)**	**0.03**	**1.54 (1.05–2.24)**	**0.03**	**1.49 (1.01–2.21)**	**0.05**
Width	**0.53 (0.37–0.76)**	**<0.001**	**0.57 (0.39–0.84)**	**0.01**	**0.50 (0.32–0.78)**	**0.002**	**0.54 (0.34–0.86)**	**0.01**
Distance to nearest 2 fibers	**1.57 (1.15–2.14)**	**0.005**	**1.47 (1.06–2.02)**	**0.02**	**1.82 (1.22–2.73)**	**0.004**	**1.70 (1.14–2.54)**	**0.009**
Box density 24 × 24 μm[b]	**0.68 (0.48–0.95)**	**0.03**	0.73 (0.52–1.04)	0.08	0.69 (0.46–1.02)	0.06	0.74 (0.50–1.09)	0.13
Box density 48 × 48 μm[b]	**0.55 (0.39–0.78)**	**<0.001**	**0.58 (0.41–0.83)**	**0.003**	**0.55 (0.36–0.82)**	**0.004**	**0.58 (0.38–0.88)**	**0.01**
Box density 96 × 96 μm[b]	**0.57 (0.41–0.79)**	**<0.001**	**0.60 (0.42–0.85)**	**0.004**	**0.55 (0.37–0.82)**	**0.003**	**0.57 (0.38–0.88)**	**0.01**
Alignment of the nearest 4 fibers	1.07 (0.78–1.46)	0.68	0.94 (0.67–1.33)	0.73	1.14 (0.79–1.64)	0.48	1.03 (0.69–1.54)	0.88
Box alignment 24 × 24 μm[c]	1.19 (0.86–1.65)	0.30	1.07 (0.77–1.51)	0.68	1.27 (0.88–1.84)	0.21	1.17 (0.80–1.72)	0.42
Distance to tumor/stromal boundary	0.84 (0.65–1.08)	0.17	0.87 (0.67–1.13)	0.29	0.87 (0.65–1.16)	0.33	0.93 (0.69–1.27)	0.66
Angle relative to tumor/stromal boundary	0.93 (0.67–1.29)	0.66	1.07 (0.75–1.52)	0.73	0.88 (0.59–1.30)	0.52	1.01 (0.65–1.55)	0.98
Composite measures[d]								
Factor 1 (high density, low alignment)	**0.72 (0.52–1.00)**	**0.05**	0.78 (0.56–1.09)	0.14	**0.68 (0.46–1.00)**	**0.05**	0.73 (0.50–1.06)	0.10
Factor 2 (high density, long distance to tumor/stromal boundary)	**0.57 (0.42–0.78)**	**<0.001**	**0.60 (0.43–0.83)**	**0.002**	**0.56 (0.39–0.82)**	**0.003**	**0.59 (0.40–0.88)**	**0.01**
Factor 3 (serpentine, not straight)	**0.68 (0.51–0.90)**	**0.01**	**0.67 (0.50–0.91)**	**0.01**	**0.68 (0.50–0.94)**	**0.02**	**0.68 (0.48–0.95)**	**0.02**
Factor 4 (high alignment, parallel orientation to tumor boundary)	0.99 (0.72–1.36)	0.95	0.86 (0.61–1.21)	0.38	1.05 (0.73–1.51)	0.80	0.92 (0.62–1.37)	0.68
Factor 5 (long, wide fibers)	**0.57 (0.41–0.81)**	**0.002**	**0.62 (0.43–0.90)**	**0.01**	**0.54 (0.36–0.82)**	**0.004**	**0.58 (0.37–0.89)**	**0.01**

Note: *P* values less than 0.05 were considered statistically significant and are indicated in bold font.

[a]Straightness is defined as the ratio of the end-to-end length to the total length of the fiber.

[b]Box density refers to the number of collagen fibers contained within box of the specified size overlaid on the fiber centroid.

[c]Alignment of fibers contained within a 24 × 24-μm box overlaid on the fiber centroid.

[d]Composite measures are linear combinations of the directly measured collagen features identified by factor analysis; see text for details.

Published OnlineFirst October 20, 2020; DOI: 10.1158/1055-9965.EPI-20-0889

95% CI, 0.42–0.85), whereas risk was elevated among DCIS cases with higher fiber straightness (HR, 1.47; 95% CI, 1.05–2.06) and distance to the nearest two fibers (HR, 1.47; 95% CI, 1.06–2.02). Total minus end-to-end length was also associated with reduced risk (HR, 0.55; 95% CI, 0.39–0.76). Fiber length, alignment, and angle relative to the tumor–stroma boundary were not associated with recurrence ($P > 0.05$). Factors 2, 3, and 5 were associated with reduced risk of any second breast cancer event (HRs ranging from 0.60 to 0.67). Hazard ratios for ipsilateral second events were similar to those for any second event. Adjustment for additional covariates had little influence on the results (Supplementary Table S3). Collagen factors were also associated with risk of contralateral second events (Supplementary Table S4).

Discussion

Our results demonstrate that numerous aspects of collagen organization around DCIS lesions are associated with DCIS pathologic characteristics and patient outcomes. Collagen fiber straightness, width, and density appear to be particularly relevant to prognosis. In addition, factor analysis identified five linear combinations of collagen fiber characteristics, representing more complex aspects of collagen organization, which were also associated with DCIS pathologic characteristics and patient outcomes. These results indicate that collagen organization should be further evaluated to provide novel insights regarding the biology of DCIS epithelial/stromal interactions and as a potential prognostic marker for breast cancer recurrence.

Previous studies of collagen organization in breast cancer have focused on collagen fiber alignment and orientation with respect to the tumor–stromal boundary. Early studies used *ex vivo* imaging of intact, unfixed mouse mammary tumors to reveal cell invasion occurring along aligned collagen fibers radiating perpendicular to the tumor–stromal boundary (36). Tumor explants cultured in a randomly organized collagen matrix led to active realignment of the collagen and migration of individual tumor cells outward along radially aligned fibers (36). Likewise, when cells were seeded into microchannels filled with random or aligned polymerized collagen, cells migrated with greater directional persistence in the aligned collagen matrices (37). In a sample of 196 human-invasive breast cancer biopsy specimens, a phenotype of perpendicularly aligned collagen fibers was identified that was associated with reduced disease-free survival (23). A subsequent study found that this phenotype did not have a statistically significant association with disease-free survival in a cohort of 371 invasive breast cancer cases, though it was associated with overall survival (24). The same study also found that collagen density in the tumor microenvironment was inversely related to risk of disease progression, consistent with our findings.

We are aware of two prior studies that have examined collagen in relation to DCIS specifically. Among 227 DCIS cases from the Wisconsin *In Situ* Cohort, greater collagen fiber angles were associated with negative hormone receptor status and presence of comedo necrosis but not with nuclear grade or disease-free survival (1). Among 776 DCIS cases in a UK cohort (38), investigators developed an image-based collagen prognostic index based on the orientation of collagen fibers relative to the DCIS boundary, fiber density, and alignment. A poor collagen prognostic index score—indicating more perpendicular fibers relative to the fiber boundary, greater fiber density, and higher alignment—was associated with higher nuclear grade, comedo-type necrosis, hormonal receptor negativity, HER2 positivity, high-proliferation index, and higher risk of recurrence. That study did not report results for fiber angle, density, and alignment individually; thus, direct comparison with our results is not possible.

As described above, prior studies have focused largely on fiber angle with respect to the tumor boundary (1, 23, 24, 38), which was not associated with outcomes in our study (nor in two of the three prior studies to directly evaluate fiber angle). We investigated a wide range of collagen fiber features. Our findings suggest that collagen fiber density is particularly relevant to DCIS pathology and outcomes. This is consistent with the Esbona and colleagues (24) study of invasive breast cancer described above, though somewhat surprising based on prior *ex vivo* mechanistic studies suggesting that collagen density was associated with increased tumor initiation and metastasis (22). This may be a reflection of differences in how collagen density was assessed, but also may indicate that the impact of collagen density may depend on other aspects of collagen organization (e.g., alignment of fibers). In addition to fiber density, fiber width, alignment, straightness, and total minus end-to-end length (another measure of straightness/curvature) were also associated with DCIS histopathology and outcomes in our study. The plasticity of the collagen matrix and its association with traditional DCIS prognostic factors (grade, necrosis) and the presence or absence of inflammation appears to follow a trend where higher nuclear grade, central necrosis, and absent inflammation are associated with less curved, less dense, narrower fibers that are further apart from one another.

Our results are also consistent with laboratory studies investigating the role of collagen in mediating the association of parity with breast cancer risk (39, 40). Maller and colleagues (40) showed that the abundance of collagen in the extracellular matrix from parous rats was associated with decreased tumor growth and reduced tumor cell invasion compared to ECM from nulliparous rats. Using methods, including SHG imaging, the authors showed that abundant collagen in the mammary glands of parous rats is less linearized, and that high-density collagen induces tumor-suppressive attributes. These results have a striking consistency with our findings, indicating that linearized/straight collagen has tumor-promoting properties whereas dense collagen is protective.

We used factor analysis to evaluate combinations of multiple collagen features. Factor identification did not use any information on recurrence, yet a number of these composite factors were indeed associated with recurrence. These factors could cluster DCIS cases into distinct phenotypes based on multiple aspects of their collagen organization. We did not identify any specific histopathologic patterns of periductal fibrosis associated with specific factors; however, some associations were plausibly explanatory. For example, one case with concentric, loosely packed wavy fibers reminiscent of unraveling or fraying rope had low scores for Factors 1, 2, and 5, a high score for Factor 4 (localized alignment) and an intermediate score for Factor 3 (curved, serpentine fibers). Further exploration of these factors may help to understand the patterns of collagen organization that are most relevant to DCIS epithelial/stromal biology and prediction of outcomes.

The biological mechanisms driving changes in collagen organization around breast cancer lesions remain unclear. Notably, our findings were robust to statistical adjustment for a number of patient characteristics, including age, menopausal status, and breast density, thereby suggesting that collagen organization is independently associated with DCIS outcomes. Future studies are required to directly evaluate a wide range of patient factors and molecular characteristics in relation to collagen organization around DCIS. Numerous pathways

Published OnlineFirst October 20, 2020; DOI: 10.1158/1055-9965.EPI-20-0889

have been identified by which cancer cells can influence collagen synthesis and organization or by which collagen can influence cancer cell behavior (41, 42). Immunohistochemical staining of DCIS specimens has revealed variability in collagen deposition and the distribution of stromal cells in the tumor microenvironment (43). The role of carcinoma-associated fibroblasts (CAF) is of particular interest as fibroblasts are important for producing collagen during mammary gland development and CAFs have been linked to breast cancer progression through various mechanisms (43). Other studies have identified stromal factors such as COX-2, CD68, and numerous extracellular matrix proteins that are correlated with collagen organization in breast cancer specimens (24, 44). Further research is needed to understand collagen-related signaling pathways involving both epithelial and stromal cells.

The multiphoton imaging approach used in our study allows for non-invasive and specific imaging of collagen fibers, and combined with quantitative image analysis tools, this provides a powerful method for assessing collagen organization (45). All fibrillar subtypes of collagen generate second harmonic signals, which comprise the majority of collagen isoforms with the notable exception of collagen type IV, a major constituent of the basement membrane. However, because the basement membrane represents a very small portion of the total collagen matrix imaged, and there are other collagen subtypes present in the basement membrane that are imaged, this exclusion should have minimal influence on our results.

We chose the risk of any subsequent event as the primary outcome in our study because women diagnosed with DCIS are concerned about their risk of any type of future breast cancer diagnosis (ipsilateral/contralateral, *in situ*/invasive). However, analyses of specific types of second events can inform our understanding of the biology and progression of DCIS related to collagen organization and could have treatment implications. We found similar risk associations for ipsilateral events as we did for the risk of any second event. Future studies with larger sample sizes are needed to specifically examine risk of ipsilateral-invasive events and contralateral events separately.

Limitations of our study include the relatively small sample size, though it was adequate for the detection of statistically significant differences in outcomes. Data on hormone receptor and HER2 status were not available for the majority of cases, because these tests were not routinely performed clinically during the time period in which most of the index DCIS cases were diagnosed. The Vermont DCIS cohort is population-based but has very limited racial diversity. Validation of our findings in external study cohorts is needed to further support the development of a collagen signature that predicts DCIS outcomes. The ability of collagen signatures to add useful information to recurrence prediction models that include other known prognostic factors should be evaluated formally. Future studies of treated and untreated women are needed to better understand the nature of the association between collagen organization and DCIS outcomes. Trials of active surveillance for DCIS should offer unique opportunities for testing prognostic markers (46–48). It is also possible that collagen organization could influence recurrence risk as a moderator of treatment effectiveness (e.g., radiotherapy or endocrine therapy).

Overall, our results demonstrate that multiple aspects of collagen organization around DCIS lesions, including collagen fiber straightness, width, and density, are associated with risk of recurrence. Collagen organization should be considered in the development of biomarker signatures to distinguish indolent from aggressive DCIS.

Authors' Disclosures

B.L. Sprague reports grants from NIH, Patient-Centered Outcomes Research Institute (PCORI), and Lake Champlain Cancer Research Organization during the conduct of the study. P.M. Vacek reports grants from NIH during the conduct of the study. S.E. Mulrow reports grants from NIH during the conduct of the study. T.A. James reports personal fees from Perimter outside the submitted work. D.L. Weaver reports grants from NIH/NCI during the conduct of the study. No disclosures were reported by the other authors.

Disclaimer

None of the funding bodies had a role in the design of the study nor the collection, analysis, or interpretation of the data, nor the writing of the article. The statements presented in this work are solely the responsibility of the authors and do not necessarily represent the official views of the NCI, the NIH, the Centers for Disease Control and Prevention, or Patient-Centered Outcomes Research Institute (PCORI), its Board of Governors, or Methodology Committee.

Authors' Contributions

B.L. Sprague: Conceptualization, data curation, supervision, funding acquisition, investigation, writing–original draft. **P.M. Vacek:** Conceptualization, data curation, formal analysis, validation, investigation, methodology, writing–review and editing. **S.E. Mulrow:** Data curation, investigation, writing–review and editing. **M.F. Evans:** Resources, data curation, investigation, writing–review and editing. **A. Trentham-Dietz:** Conceptualization, investigation, writing–review and editing. **S.D. Herschorn:** Conceptualization, data curation, investigation, writing–review and editing. **T.A. James:** Conceptualization, investigation, writing–review and editing. **N. Surachaicharn:** Resources, data curation, methodology, writing–review and editing. **A. Keikhosravi:** Resources, data curation, methodology, writing–review and editing. **K.W. Eliceiri:** Conceptualization, resources, investigation, methodology, writing–review and editing. **D.L. Weaver:** Conceptualization, resources, data curation, supervision, funding acquisition, validation, investigation, methodology, writing–review and editing. **M.W. Conklin:** Conceptualization, resources, data curation, formal analysis, supervision, funding acquisition, investigation, visualization, methodology, writing–review and editing.

Acknowledgments

This work was supported by the NCI [grant numbers U01 CA196383 and U54 CA163303 (to B.L. Sprague and D.L. Weaver), P01 CA154292 (to B.L. Sprague), R01 CA199996 (to M.W. Conklin), and P30 CA014520 (to A. Trentham-Dietz)], the Patient-Centered Outcomes Research Institute (PCORI; grant number PCS-1504–30370; to B.L. Sprague), and the University of Vermont Cancer Center with funds generously awarded by the Lake Champlain Cancer Research Organization (pilot grant #032800; to B.L. Sprague). The collection of Vermont Cancer Registry data used in this study was supported by the Centers for Disease Control and Prevention (Cooperative Agreement No. NU58DP006322 to the Vermont State Agency for Human Services). The authors wish to thank Drs. Andrew Goodwin, Brenda Waters, and Jill Warrington, who participated in the centralized review of DCIS specimens; Alison Johnson and Jennifer Kachajian at the Vermont Cancer Registry; and Denis Nunez, Rachael Chicoine, John Mace, Mark Bowman, Mike Butler, Meghan Farrington, Cindy Groseclose, Kathleen Howe, Dawn Pelkey, Dusty Quick, and Tiffany Sharp, who conduct and support data collection within the Vermont Breast Cancer Surveillance System. They also thank Drs. Yuming Liu, Bin Li, and Jeremy Bredfeldt for technical support for SHG image analysis and image collection. The authors particularly would like to acknowledge the immeasurable contribution of the late Dr. Patti Keely to this project and for her impact on the field of the science of the tumor microenvironment and the role of collagen in tumor progression that motivated this study.

The costs of publication of this article were defrayed in part by the payment of page charges. This article must therefore be hereby marked *advertisement* in accordance with 18 U.S.C. Section 1734 solely to indicate this fact.

Received June 9, 2020; revised August 25, 2020; accepted October 9, 2020; published first October 20, 2020.

Published OnlineFirst October 20, 2020; DOI: 10.1158/1055-9965.EPI-20-0889

References

1. Conklin MW, Gangnon RE, Sprague BL, Van Gemert L, Hampton JM, Eliceiri KW, et al. Collagen alignment as a predictor of recurrence after ductal carcinoma in situ. Cancer Epidemiol Biomarkers Prev 2018;27:138–45.
2. Miglioretti DL, Zhu W, Kerlikowske K, Sprague BL, Onega T, Buist DS, et al. Breast tumor prognostic characteristics and biennial vs annual mammography, age, and menopausal status. JAMA Oncol 2015;1:1069–77.
3. Sprague BL, McLaughlin V, Hampton JM, Newcomb PA, Trentham-Dietz A. Disease-free survival by treatment after a DCIS diagnosis in a population-based cohort study. Breast Cancer Res Treat 2013;141:145–54.
4. Duffy SW, Agbaje O, Tabar L, Vitak B, Bjurstam N, Bjorneld L, et al. Overdiagnosis and overtreatment of breast cancer: estimates of overdiagnosis from two trials of mammographic screening for breast cancer. Breast Cancer Res 2005;7:258–65.
5. Ernster VL, Barclay J. Increases in ductal carcinoma in situ (DCIS) of the breast in relation to mammography: a dilemma. J Natl Cancer Inst Monogr 1997:151–6.
6. Esserman L, Shieh Y, Thompson I. Rethinking screening for breast cancer and prostate cancer. JAMA 2009;302:1685–92.
7. Betsill WL Jr, Rosen PP, Lieberman PH, Robbins GF. Intraductal carcinoma: long-term follow-up after treatment by biopsy alone. JAMA 1978; 239:1863–7.
8. Rosen PP, Braun DW Jr, Kinne DE. The clinical significance of pre-invasive breast carcinoma. Cancer 1980;46:919–25.
9. Page DL, Dupont WD, Rogers LW, Landenberger M. Intraductal carcinoma of the breast: follow-up after biopsy only. Cancer 1982;49:751–8.
10. Eusebi V, Feudale E, Foschini MP, Micheli A, Conti A, Riva C, et al. Long-term follow-up of in situ carcinoma of the breast. Semin Diagn Pathol 1994; 11:223–35.
11. Groen EJ, Elshof LE, Visser LL, Rutgers EJT, Winter-Warnars HAO, Lips EH, et al. Finding the balance between over- and under-treatment of ductal carcinoma in situ (DCIS). Breast 2017;31:274–83.
12. Hwang ES, Esserman LJ. Management of ductal carcinoma in situ. Surg Clin North Am 1999;79:1007–30.
13. van de Vijver MJ, He YD, van't Veer LJ, Dai H, Hart AA, Voskuil DW, et al. A gene-expression signature as a predictor of survival in breast cancer. N Engl J Med 2002;347:1999–2009.
14. van't Veer LJ, Dai H, van de Vijver MJ, He YD, Hart AA, Mao M, et al. Gene expression profiling predicts clinical outcome of breast cancer. Nature 2002;415: 530–6.
15. Solin LJ, Gray R, Baehner FL, Butler SM, Hughes LL, Yoshizawa C, et al. A multigene expression assay to predict local recurrence risk for ductal carcinoma in situ of the breast. J Natl Cancer Inst 2013;105:701–10.
16. Hwang ES, DeVries S, Chew KL, Moore DH II, Kerlikowske K, Thor A, et al. Patterns of chromosomal alterations in breast ductal carcinoma in situ. Clin Cancer Res 2004;10:5160–7.
17. Ronnov-Jessen L, Bissell MJ. Breast cancer by proxy: can the microenvironment be both the cause and consequence? Trends Mol Med 2009;15:5–13.
18. Mueller MM, Fusenig NE. Friends or foes—bipolar effects of the tumour stroma in cancer. Nat Rev Cancer 2004;4:839–49.
19. Bhowmick NA, Neilson EG, Moses HL. Stromal fibroblasts in cancer initiation and progression. Nature 2004;432:332–7.
20. Wiseman BS, Werb Z. Stromal effects on mammary gland development and breast cancer. Science 2002;296:1046–9.
21. Sgroi DC. Preinvasive breast cancer. Annu Rev Pathol 2010;5:193–221.
22. Provenzano PP, Inman DR, Eliceiri KW, Knittel JG, Yan L, Rueden CT, et al. Collagen density promotes mammary tumor initiation and progression. BMC Med 2008;6:11.
23. Conklin MW, Eickhoff JC, Riching KM, Pehlke CA, Eliceiri KW, Provenzano PP, et al. Aligned collagen is a prognostic signature for survival in human breast carcinoma. Am J Pathol 2011;178:1221–32.
24. Esbona K, Yi Y, Saha S, Yu M, Van Doorn RR, Conklin MW, et al. The presence of cyclooxygenase 2, tumor-associated macrophages, and collagen alignment as prognostic markers for invasive breast carcinoma patients. Am J Pathol 2018; 188:559–73.
25. Sprague BL, Vacek PM, Herschorn SD, James TA, Geller BM, Trentham-Dietz A, et al. Time-varying risks of second events following a DCIS diagnosis in the population-based Vermont DCIS cohort. Breast Cancer Res Treat 2019;174:227–35.
26. Lehman CD, Arao RF, Sprague BL, Lee JM, Buist DS, Kerlikowske K, et al. National performance benchmarks for modern screening digital mammography: update from the Breast Cancer Surveillance Consortium. Radiology 2017; 283:49–58.
27. Ballard-Barbash R, Taplin SH, Yankaskas BC, Ernster VL, Rosenberg RD, Carney PA, et al. Breast Cancer Surveillance Consortium: a national mammography screening and outcomes database. AJR Am J Roentgenol 1997;169:1001–8.
28. Sprague BL, Bolton KC, Mace JL, Herschorn SD, James TA, Vacek PM, et al. Registry-based study of trends in breast cancer screening mammography before and after the 2009 U.S. Preventive Services Task Force recommendations. Radiology 2014;270:354–61.
29. Geller B, Worden J, Ashley J, Oppenheimer R, Weaver D. Multipurpose statewide breast cancer surveillance system: the Vermont experience. J Reg Manage 1996;23:168–74.
30. Sickles EA, d'Orsi CJ, Bassett LW, Appleton CM, Berg WA, Burnside ES. ACR BI-RADS—mammography. 5th edition. In: ACR BI-RADS atlas: breast imaging reporting and data system. Reston (VA): American College of Radiology; 2013.
31. Liu Y, Keikhosravi A, Mehta GS, Drifka CR, Eliceiri KW. Methods for quantifying fibrillar collagen alignment. Methods Mol Biol 2017;1627:429–51.
32. Bredfeldt JS, Liu Y, Pehlke CA, Conklin MW, Szulczewski JM, Inman DR, et al. Computational segmentation of collagen fibers from second-harmonic generation images of breast cancer. J Biomed Opt 2014;19:16007.
33. Keikhosravi A, Li B, Liu Y, Eliceiri KW. Intensity-based registration of bright-field and second-harmonic generation images of histopathology tissue sections. Biomed Opt Express 2020;11:160–73.
34. Bredfeldt JS, Liu Y, Conklin MW, Keely PJ, Mackie TR, Eliceiri KW. Automated quantification of aligned collagen for human breast carcinoma prognosis. J Pathol Inform 2014;5:28.
35. Liu Y, Keikhosravi A, Pehlke CA, Bredfeldt JS, Dutson M, Liu H, et al. Fibrillar collagen quantification with curvelet transform based computational methods. Front Bioeng Biotechnol 2020;8:198.
36. Provenzano PP, Eliceiri KW, Campbell JM, Inman DR, White JG, Keely PJ. Collagen reorganization at the tumor-stromal interface facilitates local invasion. BMC Med 2006;4:38.
37. Riching KM, Cox BL, Salick MR, Pehlke C, Riching AS, Ponik SM, et al. 3D collagen alignment limits protrusions to enhance breast cancer cell persistence. Biophys J 2014;107:2546–58.
38. Toss MS, Miligy IM, Gorringe KL, AlKawaz A, Mittal K, Aneja R, et al. Geometric characteristics of collagen have independent prognostic significance in breast ductal carcinoma in situ: an image analysis study. Mod Pathol 2019;32:1473–85.
39. Lyons TR, O'Brien J, Borges VF, Conklin MW, Keely PJ, Eliceiri KW, et al. Postpartum mammary gland involution drives progression of ductal carcinoma in situ through collagen and COX-2. Nat Med 2011;17:1109–15.
40. Maller O, Hansen KC, Lyons TR, Acerbi I, Weaver VM, Prekeris R, et al. Collagen architecture in pregnancy-induced protection from breast cancer. J Cell Sci 2013; 126:4108–10.
41. Xu S, Xu H, Wang W, Li S, Li H, Li T, et al. The role of collagen in cancer: from bench to bedside. J Transl Med 2019;17:309.
42. Conklin MW, Keely PJ. Why the stroma matters in breast cancer: insights into breast cancer patient outcomes through the examination of stromal biomarkers. Cell Adh Migr 2012;6:249–60.
43. Nelson AC, Machado HL, Schwertfeger KL. Breaking through to the other side: microenvironment contributions to DCIS initiation and progression. J Mammary Gland Biol Neoplasia 2018;23:207–21.
44. Yang N, Mosher R, Seo S, Beebe D, Friedl A. Syndecan-1 in breast cancer stroma fibroblasts regulates extracellular matrix fiber organization and carcinoma cell motility. Am J Pathol 2011;178:325–35.
45. Chen X, Nadiarynkh O, Plotnikov S, Campagnola PJ. Second harmonic generation microscopy for quantitative analysis of collagen fibrillar structure. Nat Protoc 2012;7:654–69.
46. Francis A, Fallowfield L, Rea D. The LORIS trial: addressing overtreatment of ductal carcinoma in situ. Clin Oncol (R Coll Radiol) 2015;27:6–8.
47. Elshof LE, Tryfonidis K, Slaets L, van Leeuwen-Stok AE, Skinner VP, Dif N, et al. Feasibility of a prospective, randomised, open-label, international multicentre, phase III, non-inferiority trial to assess the safety of active surveillance for low risk ductal carcinoma in situ—the LORD study. Eur J Cancer 2015;51:1497–510.
48. Hwang ES, Hyslop T, Lynch T, Frank E, Pinto D, Basila D, et al. The COMET (comparison of operative versus monitoring and endocrine therapy) trial: a phase III randomised controlled clinical trial for low-risk ductal carcinoma in situ (DCIS). BMJ Open 2019;9:e026797.

Published OnlineFirst October 20, 2020; DOI: 10.1158/1055-9965.EPI-20-0889

Cancer Epidemiology, Biomarkers & Prevention

AACR American Association for Cancer Research

Collagen Organization in Relation to Ductal Carcinoma *In Situ* Pathology and Outcomes

Brian L. Sprague, Pamela M. Vacek, Sophie E. Mulrow, et al.

Cancer Epidemiol Biomarkers Prev 2021;30:80-88. Published OnlineFirst October 20, 2020.